JOURNAL OF APPLIED ELECTROCHEMISTRY **27** (1997) 756–761

Iron deposition from a $FeCl_2$ solution containing suspended silicon particles

A. HOVESTAD, R. ANSINK, L. J. J. JANSSEN

Faculty of Chemical Engineering, Eindhoven University of Technology, PO Box 513, 5600 MB Eindhoven, The Netherlands

Received 15 April 1996; revised 3 February 1997

The effect of suspended Si particles on Fe deposition from a $FeCl_2$ solution was investigated. The conductivity of a $FeCl_2$ solution in the presence of suspended Si particles was found to be consistent with the Bruggeman theory and its viscosity shows Newtonian behaviour. The Fe^{3+} mass transfer to a rotating disc electrode in the presence of Si particles increases with Si content in the solution at higher rotation speeds. The cathodic polarization curves shift to slightly lower potentials and the Fe deposition current efficiency increases with increasing Si concentration. These changes are related to an increase in the rate of Fe deposition on Fe with Si particle content in the solution. Finally, Si embedment in the Fe increases with current density between 0.25 and 2 kA m^{-2}.

List of symbols

$c_{b,i}$	bulk concentration of species i (mol m^{-3})
D_i	diffusion coefficient of species i (m^2 s^{-1})
E	electrode potential (V)
f	F/RT (V^{-1})
F	Faraday constant (C mol^{-1})
j	current density (A m^{-2})
j_0	exchange current density (A m^{-2})
$j_{L,i}$	limiting current density of species i (A m^{-2})
j_m	modified current density, $j/(1-\exp(\alpha n f\lvert\eta\rvert))$ (A m^{-2})
n	number of electrons transferred for the oxidation or reduction of an ion
p_ϕ	exponent to ω for particle volume fraction ϕ
q	charge (C)
R	gas constant (J K^{-1} mol^{-1})
R_Ω	ohmic resistance (Ω)
T	temperature (K)
Z_{Re}	real part of electrode impedance (Ω)

Greek letters

α	cathodic transfer coefficient
Γ	current efficiency
η	overpotential (V)
κ	conductivity (S m^{-1})
μ	viscosity (Pa s)
$[\mu]$	intrinsic viscosity
ϕ	particle volume fraction
ϕ_m	maximum particle volume fraction
ω	angular velocity of rotating disc electrode (s^{-1})

subscripts

c	continuous phase
s	suspension
r	reduced
–	cathodic
+	anodic

1. Introduction

Iron core transformers suffer appreciable magnetic energy losses due to eddy currents. Using stacks of thin sheets (< 0.1 mm) of highly pure Fe alloyed with 5–7 wt % of Si as the transformer core may minimize these losses. Although Fe–Si alloys can be easily prepared, they are too brittle to be rolled to thin sheets. Since, electrodeposition allows the production of very thin sheets of high purity, electrochemical codeposition of Si particles in an Fe matrix is investigated as a method of making transformer sheet. In a subsequent heat treatment the dispersion of Si in Fe interdiffuses to produce a homogeneous alloy. A similar method has been reported by Bazzard and Boden for the preparation of Ni–Cr alloys [1] and by Smith *et al.* for Fe–Ni–Cr [2] alloys.

Electrochemical codeposition of particles in a metal matrix involves the incorporation of inert particles, suspended in a metal plating solution, in an electrochemically grown metal [3–5]. Although, a wide range of particle–metal systems has been investigated, the mechanism of the codeposition process is still not fully understood [3–5]. In all the proposed mechanisms the metal deposition is considered to be unaffected by the presence of particles. However, several researchers have reported marked changes in the metal deposition behaviour on addition of particles, which are closely coupled to codeposition features [6–12]. Among others a shift in the

cathodic polarization curve, changes in cathodic Tafel slopes and decreases in metal deposition current efficiency have been observed. Further investigations on metal deposition in the presence of suspended particles are required to obtain a better understanding of these effects and their relation to the codeposition mechanism. Knowledge of such effects is also necessary for successful industrial application of codeposition systems. In the present work the physical and electrochemical behaviour of a Fe plating bath in the presence of suspended Si particles has been determined.

2. Experimental details

A 3 M $FeCl_2$ solution, operating at 90 °C and pH 1, was used as the Fe plating bath. Before each series of experiments a fresh solution was prepared with $FeCl_2.4H_2O$ (Merck, extra pure) and Fe powder (Goodfellow, 99% pure) was added. This solution was allowed to stand in the presence of Fe powder to reduce ferric ions, present as impurity in the salt. Despite this pretreatment, traces of ferric ions, about 3–5 mM, were still present in the $FeCl_2$ solution during the measurements. Two types of anisotropic Si particles were used. Their specifications are given in Table 1. Type I was used to measure all reported parameters. Additionally, the electrochemical experiments were repeated using type II.

The conductivity of the suspensions was determined under continuous stirring using a conductivity cell (Philips PW9550/60) and a conductivity meter (Radiometer CDM2). A viscosity meter (Ubbelohde, type 0c) was used to measure the viscosity.

The electrochemical experiments were performed in a three-compartment cell consisting of a 150 cm^3 thermostated vessel for the working electrode, a counter electrode compartment and a Luggin capillary compartment for the reference electrode. A gas inlet and outlet were connected to the working electrode compartment. Two types of rotating disc electrodes (RDE), namely a Pt-RDE and a RDE holding interchangeable Ti cups, were used both having an active surface area of 0.38 cm^2. A low alloy steel plate was used as the counter electrode in the experiments involving Fe deposition, while a Pt-plate counter electrode was used in the mass transfer measurements. All potentials are referred to a saturated calomel electrode (SCE), which was used as reference.

Before the experiments the electrolyte was saturated with nitrogen and electrochemically pretreated for 90 min at −0.1 A using a 10 cm^2 Ti cathode and a low alloy steel anode. During the experiments nitrogen was passed over the electrolyte to exclude oxygen. In the period between successive measurements a magnetic stirrer was used to maintain the Si particles in suspension. The time scale of the measurements was such that during measurements the electrode rotation was sufficient to prevent particle settlement. All measurements were controlled and registered by a computer coupled to an Autolab/PGSTAT20 (ECO Chemie). Impedance measurements were carried out with a Solatron 1250 frequency response analyser and a Solatron electrochemical interface 1286.

The current efficiency of Fe deposition, Γ_{Fe}, was obtained by measuring the charge, q_-, consumed during 30 min of cathodic polarization and subsequently the charge, q_+, necessary for complete anodic dissolution of the deposited Fe. The charge q_- was corrected for the charge $q_{-,Fe^{3+}}$ used for reduction of Fe^{3+} to Fe^{2+} and $\Gamma_{Fe} = q_+/(q_- - q_{-,Fe^{3+}})$ was calculated. It was found that during the potentiostatic deposition a steady current was reached within a few minutes. The dissolution was carried out a 0 V vs SCE to exclude interference of hydrogen evolution and Fe^{2+} oxidation. Side reactions, like the reduction of traces Fe^{3+}, were negligible at this potential. The Fe deposition was preceded by a conditioning period of 10 min at 0 V vs SCE and a short nucleation pulse (1 s) at −0.85 V vs SCE.

Cathodic polarization curves for Fe deposition and limiting currents for Fe^{3+} reduction were obtained by cyclic voltammetry. Before each measurement a conditioning potential of 0 V vs SCE was applied for 5 min. Some irreproducibility was noticed in the cathodic polarization curves and in the Fe^{3+} reduction limiting currents. Therefore, the effect of particles was investigated by progressively adding fixed quantities of Si powder to the same solution. After each addition of Si powder the solution was magnetically stirred for 5 min to obtain a homogeneous suspension. After each measurement of a cathodic voltammogram, potentiostatic impedance spectra were recorded at several cathodic potentials in the frequency range 1 to 65 000 Hz to obtain the ohmic solution resistance.

Galvanostatic deposition experiments using the Ti-RDE were performed to determine the Si incorporation in Fe as a function of the current density. The deposits were weighed and dissolved in dilute HNO_3 in a Pt crucible. After evaporation to dryness the Si was dissolved in 1.2 g $NaCO_3$ and 0.4 g $NaB_4O_7.10H_2O$ at 1000 °C for 30 min. The resulting mixture was dissolved in 2 M HCl and spectrophotometrically analysed for Si using the heteropoly blue method [13].

Table 1. Properties of the Si particles

Type	*Purity* /% Si	*Average size* /μm
I	97.5	1.1 (by number)
II	99.3	3.2 (by volume)

3. Results and discussion

3.1. *Conductivity and viscosity*

Experiments on suspensions of glass beads containing a broad range of particle sizes carried out by De La

Rue and Tobias [14] indicate that Bruggeman's equation, namely,

$$\frac{\kappa_s}{\kappa_c} = (1-\phi)^{3/2} \quad (1)$$

represents the dependence of the suspension conductivity, κ_s, on the particle volume fraction, ϕ, satisfactorily. The conductivity of the continuous phase is indicated by κ_c. The experimental results for the reduced conductivity $\kappa_r = \kappa_s/\kappa_c$ of the 3 M $FeCl_2$–Si suspensions are given in Fig. 1. The solid line in this Figure represents the Bruggeman relation, which fits the experimental values for κ_s/κ_c very well. Hence, the 3 M $FeCl_2$ solution containing Si particles behaves like a suspension of nonconducting particles.

Dispersed particles often cause non-Newtonian viscous behaviour, which influences the hydrodynamics and mass transfer in suspensions. The reduced suspension viscosity (μ_r), that is the suspension viscosity divided by the viscosity of the continuous phase, is given by the Krieger–Dougherty equation [15]:

$$\mu_r = \left(1 - \frac{\phi}{\phi_m}\right)^{-[\mu]\phi_m} \quad (2)$$

where $[\mu] = (\mu_r - 1)/\phi$ is the intrinsic viscosity, which is 2.5 for spherical particles and ϕ_m is the maximum particle volume fraction. In Fig. 2 the experimental results for μ_r against ϕ_{Si} are given. These results fit the Krieger–Dougherty equation taking $[\mu] = 3.2$ and $\phi_m = 1.05$, which is represented by the full line in Fig. 2. The value of $[\mu]$ being higher than 2.5 agrees with the fact that the Si particles are anisotropic [15]. Since the investigated suspensions are relatively dilute the value of ϕ_m cannot be determined accurately and has an unrealistic value. It can be concluded that the 3 M $FeCl_2$–Si suspension behaves as a Newtonian fluid.

3.2. *Particle type*

Two types of Si particle were used in the electrochemical experiments (Table 1) The type I particles have a much broader range of particle size than the type II particles. Both types of particle showed the same effect on the parameters reported below. Therefore, only the results obtained for the type II particles will be shown.

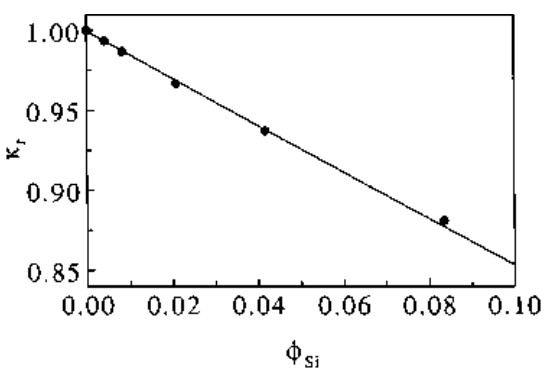

Fig. 1. Reduced conductivity κ_r (●) of a 3 M $FeCl_2$ solution at 363 K as a function of Si particle volume fraction. Solid line represents Bruggeman equation.

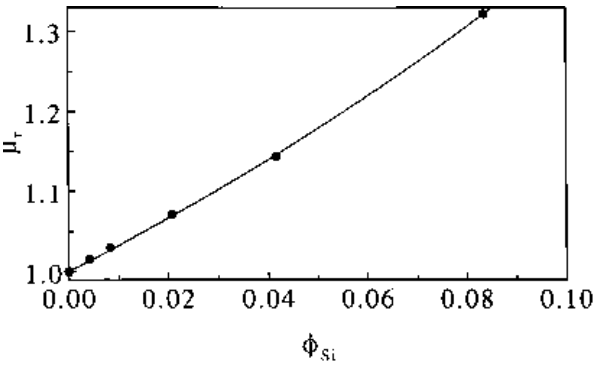

Fig. 2. Reduced viscosity μ_r (●) of a 3 M $FeCl_2$ solution at 363 K as a function of Si particle volume fraction. Solid line represents fitted Krieger–Dougherty equation.

3.3. *Mass transfer*

It is well-known that suspended inert particles can enhance ionic mass transfer to electrodes [16–21]. The mass transfer enhancement may play a role in the effects of particles on metal deposition. The effect of Si particles on the ionic mass transfer in a 3 M $FeCl_2$ solution was determined using Fe^{3+} as indicator ion. In a series of experiments voltammograms at various rotation speeds of a Pt-RDE were measured to determine the limiting current for Fe^{3+} reduction in a 3 M $FeCl_2$ solution containing a small quantity of $FeCl_3$ and various amounts of Si particles.

Starting with a particle-free 3 M $FeCl_2$ solution containing 0.037 M $FeCl_3$, the open-circuit potential (o.c.p.) of the Pt-electrode became more positive after each addition of Si particles due to a decrease in Fe^{3+} concentration. This decrease is caused by the reaction of Fe^{3+} with metallic Fe, present as an impurity in the Si powder. The Fe^{3+} concentration became constant at a lower level soon after addition of Si particles. Hence, to determine the effect of Si particles on the Fe^{3+} mass transfer accurately, a correction for the decrease in Fe^{3+} concentration was made. The relation between the o.c.p. and $c_{b,Fe^{3+}}$ was determined in a particle-free 3 M $FeCl_2$ solution and it was found that the o.c.p. was given by the Nernst equation. Hence, the Fe^{3+} concentration in the presence of particles was calculated from the measured o.c.p.

It was found that the limiting current density, $j_{L,Fe^{3+}}$, for Fe^{3+} reduction is proportional to ω^{p_ϕ}. The values for p_ϕ were obtained from the slope of $\log j_{L,Fe^{3+}}$ against $\log \omega$ curves and are presented in Table 2. In the absence of Si particles $p_\phi = 0.5$, the same value as for the Levich equation [22]. Applying the Levich equation it was found that $D_{Fe^{3+}} = 1.2 \times 10^{-9}\ m^2\ s^{-1}$ in 3 M $FeCl_2$ at 363 K.

In Fig. 3 $j_{L,Fe^{3+}}/c_{b,Fe^{3+}}$ is plotted against ϕ_{Si} for various rotation speeds. This shows that at rotation

Table 2. Exponents of the ω dependence of the Fe^{3+} limiting current density in a 3 M $FeCl_2$ solution at 363 K in the presence of various amounts of Si particles

ϕ_{Si}	p_ϕ
0	0.50
0.004	0.50
0.009	0.50
0.021	0.51
0.043	0.53
0.086	0.54
0.172	0.60

speeds $\omega < 16$ rps the Fe^{3+} mass transfer coefficient is practically independent of ϕ_{Si} and at $\omega \geq 16$ rps it increases almost linearly with ϕ_{Si}. This is the typical behaviour reported for ionic mass transfer in the presence of suspended particles [16–21]. However, the increase in Fe^{3+} mass transfer coefficient is clearly smaller compared to values reported in the literature [16–21]. Furthermore, an increase in the exponent p_ϕ with ϕ similar to that shown for ϕ_{Si} in Table 2, was reported by Sonneveld et al. [19] and Caprani et al. [16].

3.4. *Current efficiency for Fe deposition*

Figure 4 shows Γ_{Fe} as a function of the current density for various Si concentrations and a rotation speed of 16 rps. All curves in Fig. 4 show an increase in efficiency up to 0.5 kA m^{-2}. Taking into account the inaccuracy of the results it can be concluded that the Fe deposition current efficiency is practically constant in the current density range 0.5 to 2.5 kA m^{-2}. Γ_{Fe} increases slightly with increasing Si concentration. In contrast to the observations for Ni–SiC [9, 12] and Ni–Al_2O_3 [11] the Si particles have no dramatic effect on the Fe deposition current efficiency. Moreover, an increase, rather than a decrease in Γ is observed in the presence of suspended particles.

3.5. *Polarization behaviour*

Voltammograms on a Pt and Ti-RDE were measured in a 3 M $FeCl_2$ solution with various Si particle contents. The obtained current densities were very high up to about 10 kA m^{-2}. A correction for the ohmic potential drop was necessary to obtain correct electrode potentials. It was found that the impedance method was the most reliable to effect this correction. Corrections obtained with the current interruption method led to overcompensation at high current densities.

Results of impedance measurements were plotted on Nyquist diagrams, which show inclined well-shaped semicircles with their centres above the real axis. Inclination of semicircles in impedance plots has often been observed and is attributed to nonuniformity of the electric field at rough electrode surfaces [23, 24]. The ohmic solution resistance between the working electrode and the tip of the Luggin capillary is given by the distance between $Z_{Re} = 0$ and the intersection point of a semicircle with the Z_{Re} axis [23, 24]. It was found that within experimental accuracy the ohmic solution resistance, R_Ω, does not change with potential within the scan range of the voltammograms.

Figure 5 shows voltammograms on a Ti and Pt-RDE rotated at 16 rps. For both electrodes the potential was scanned at a rate of 2.5 mV s^{-1} from -0.5 V to a more negative potential and back. The ohmic potential drop was taken into account to obtain the correct electrode potentials for the volta-

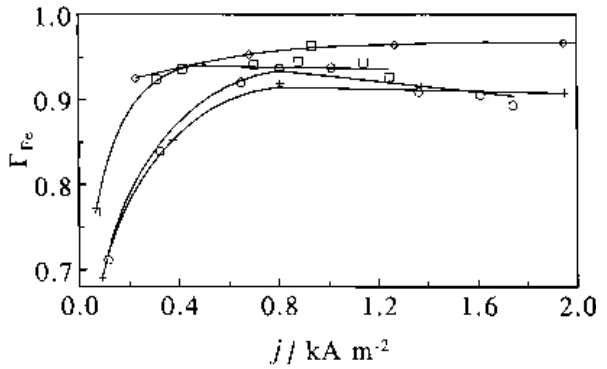

Fig. 4. Fe deposition current efficiency as function of current density in a 3 M $FeCl_2$ solution at 363 K containing various amounts of Si particles, ϕ_{Si}: 0 (+), 0.004 (○) 0.086 (□) and 0.172 (◇).

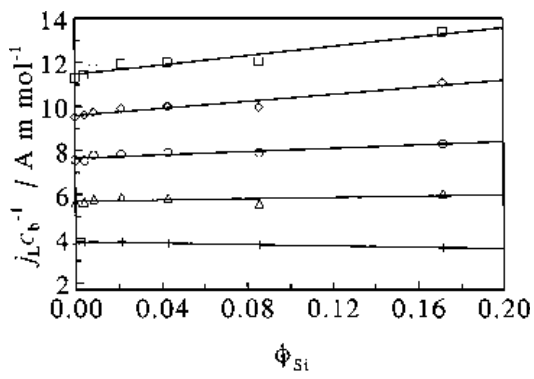

Fig. 3. Concentration normalized limiting current density for Fe^{3+} reduction at a Pt-RDE in a 3 M $FeCl_2$ solution at 363 K as a function of ϕ_{Si} at different RDE rotation speeds, ω: 4 (+), 9 (△); 16 (○); 25 (◇) and 36 rps (□).

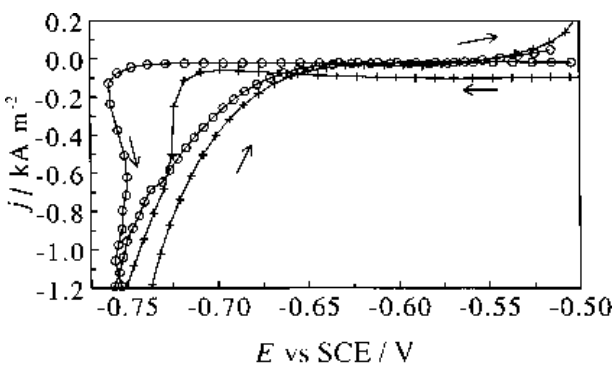

Fig. 5. Voltammograms for Fe deposition on a Pt-RDE (+) and a Ti-RDE (○) from a particle-free 3 M $FeCl_2$ solution at 363 K. Potential scan rate 2.5 mV s^{-1}; RDE rotation speed 16 rps. Arrows indicate scan direction.

mmograms. Both voltammograms show a strong hysteresis between the cathodic and anodic scan, indicating the occurrence of a crystallization overpotential. This is supported by current efficiency measurements. It was found that, at −0.75 V, Fe deposits on Ti with 2.5% current efficiency, while after a nucleation pulse Fe deposits on Fe with 50% current efficiency. It follows from Fig. 5 that the current density in the cathodic scan remains constant from −0.50 V to −0.72 V and −0.77 V, for Pt and Ti, respectively. At more cathodic potentials the Fe deposition current rises sharply. This shows that there is a clear difference in crystallization overpotential for Fe deposition on Pt and Ti.

Addition of various amounts of Si to the 3 M $FeCl_2$ solution does not significantly change the value of the crystallization overpotential for Fe deposition on Pt as well as on Ti. Thus, a strong decrease in the crystallization overpotential, as reported for Ni–SiC [9] and Ni–Cr [10] codeposition, does not take place in the Fe–Si system.

The anodic scans measured on Pt at various volume fractions of Si particles are plotted in Fig. 6. On addition of Si particles the cathodic polarization curve for Fe deposition shifts to slightly lower overpotentials. This was found for both the anodic and cathodic scans on Pt as well as on Ti. A similar depolarization has been reported for several metal particle systems [6–10]. Taking into account the increase in Γ_{Fe} with ϕ_{Si} (Fig. 4), it can be concluded that the presence of Si particles in the 3 M $FeCl_2$ solution decreases the overpotential for Fe deposition on Fe compared to the particle-free solution. Since it is unlikely that the Fe deposition reaction is mass transfer controlled in the current density range considered and Si particles hardly affect the mass transfer, the depolarization is not due to Fe^{2+} mass transfer enhancement by Si particles. The decrease in overpotential indicates a slight change in the kinetic parameters for Fe deposition with ϕ_{Si}.

To determine the kinetic parameters for Fe deposition on Fe modified Tafel plots were used. By rearrangement of the Butler–Volmer equation it can be shown that $j_{m,Fe} = j_{Fe}/(1 - \exp(-nf|\eta|)) = j_{0,Fe} \exp$

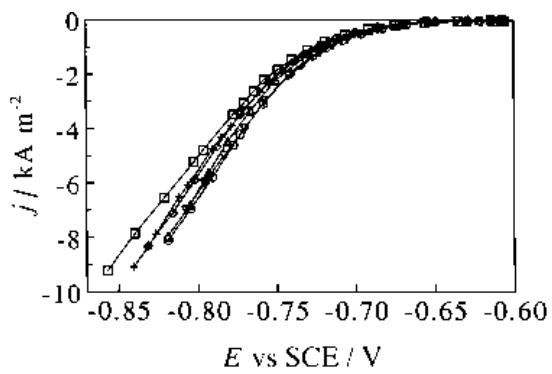

Fig. 6. Voltammograms for Fe deposition on a Pt-RDE from a 3 M $FeCl_2$ solution at 363 K containing various amounts of Si particles. Potential scan rate 2.5 mV s^{-1}; RDE rotation speed 16 rps. ϕ_{Si}: 0 (□), 0.004 (+), 0.009 (◇), 0.043 (△), 0.086 (○) and 0.172 (▽).

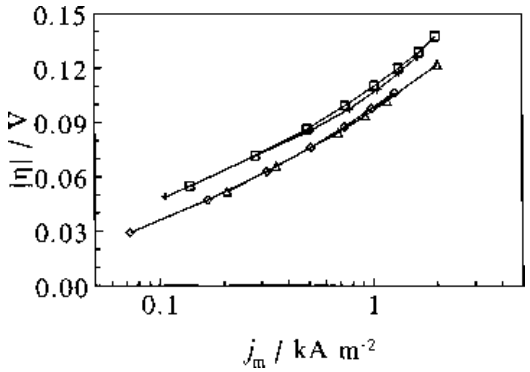

Fig. 7. Modified Tafel plots for Fe deposition on a Pt-RDE from a 3 M $FeCl_2$ solution at 363 K containing various amounts of Si particles. RDE rotation speed 16 rps. ϕ_{Si}: 0 (□), 0.004 (+), 0.086 (◇) and 0.172 (△).

$(\alpha nf|\eta|)$. The current density for Fe deposition $j_{Fe} = \Gamma_{Fe} j$. In Fig. 7 the modified Tafel plot of log $j_{m,Fe}$ against $|\eta|$ is given. Fig. 7 shows that the modified Tafel slope increases with increasing overpotential. This dependence may be explained either by the crystallization potential or the activation polarization due to the electron transfer reaction. In the latter case a change in the nature of the electrode surface may be occurring, for example caused by the formation of iron hydrides.

The modified Tafel slope is practically independent of the Si particle content. The observed modified Tafel slope at $|\eta| < 0.075$ V, namely 0.062 V agrees with the results reported for Fe deposition from $FeSO_4$ solutions [25, 26]. Assuming $n = 1$ it can be calculated that $\alpha = 1.1$, which deviates from $\alpha = 0.5$ usually found for a slow one-electron electrode reaction [25, 26]. Linear extrapolation of the modified Tafel curve to $\eta = 0$ gives $j_{0,Fe}$ if the electron transfer is the rate-determining step. In this case $j_{0,Fe} = 0.015$ kA m^{-2} for the particle free solution and $j_{0,Fe}$ increases slightly with increasing ϕ_{Si}. Thus, Si particles enhance the rate of Fe deposition on Fe, which results in higher deposition current efficiencies and lower overpotentials.

3.6. *Codeposition*

The Si codepositing with Fe in a 3 M $FeCl_2$ solution containing 0.086 volume fraction Si particles was determined for various current densities using a Ti-RDE rotating at 16 rps. In Fig. 8 the amount of Si embedded in the Fe matrix is given as a function of the current density and is seen to increase with current density. In contrast to various other codeposition systems [3–6, 11] no maxima are found for Si embedment within the investigated current density range. At a current density of 2 kA m^{-2} the desired Fe–Si composite containing ~ 5 wt % Si particles can be obtained.

Webb *et al.* [11] observed marked changes in the deposition current efficiency and cathodic polarization curves for Ni–Al_2O_3 codeposition, which depend on the amount of embedded Al_2O_3 particles. Taking into account the practically constant value of Γ_{Fe}

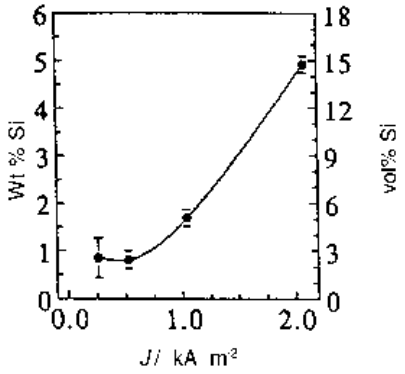

Fig. 8. Si particle embedment in Fe deposited on a Pt-RDE from a 3 M $FeCl_2$ solution at 363 K containing 0.086 volume fraction Si particles as a function of current density. RDE rotation speed 16 rps.

above 0.5 kA m^{-2}, the amount of Si embedded in Fe does not affect the Fe deposition current efficiency. Moreover, there is no effect of the amount of embedded Si particles on the polarization curves for Fe deposition. The observed effects on Γ_{Fe} and the cathodic polarization curves are relatively small and are related to the amount of suspended Si particles.

Acknowledgement

This research was financially supported by the Packaging Technology, Electrochemical Surface Technology department headed by G.C. van Haastrecht of Hoogovens Research and Development IJmuiden.

References

[1] R. Bazzard and P. J. Boden, *Trans. Inst. Met. Finish.* **50** (1972) 207.
[2] G. R. Smith, J. E. Allison, Jr. and W. J. Kolodrubetz, *Electrochem. Soc. Ext. Abstr.* **85-2** (1985) 326.
[3] C. Buelens, J. Fransaer, J. P. Celis and J. R. Roos, *Bull. Electrochem.* **8** (1992) 371.
[4] J. Fransaer, J. P. Celis and J. R. Roos, *Met. Finish.* **91** (1993) 97.
[5] A. Hovestad, L. J. J. Janssen, *J. Appl. Electrochem.* **25** (1995) 519.
[6] C. Buelens. J. P. Celis and J. R. Roos, *ibid.* **13** (1983) 541.
[7] Y. Suzuki, M. Wajima and O. Asai, *J. Electrochem. Soc.* **133** (1986) 259.
[8] E. A. Lukashev, *Russ. J. Electrochem.* **30** (1994) 83.
[9] S. W. Watson, *J. Electrochem. Soc.* **140** (1993) 2235.
[10] S. W. Watson and R. P. Walters, *ibid.* **138** (1991) 3633.
[11] P. R. Webb and N. L. Robertson, *ibid.* **141** (1994) 699.
[12] S. H. Yeh and C. C. Wan, *J. Appl. Electrochem.* **24** (1994) 993.
[13] D. F. Boltz, L. A. Trudell and G. V. Potter, *in* 'Colorimetric Determination of Nonmetals'; Chemical Analysis Vol. 8, 2nd edn (edited by D. F. Boltz and J. A. Howell), J. Wiley & Sons, New York (1978), p. 442.
[14] R. E. De La Rue and C. W. Tobias, *J. Electrochem. Soc.* **106** (1959) 827.
[15] H. A. Barnes, J. F. Hutton and K. Walters, 'An Introduction to Rheology', Elsevier, Amsterdam (1989), p. 115.
[16] M. Marie de Ficquelmont-Loizos, L. Tamisier and A. Caprani, *J. Electrochem. Soc.* **135** (1988) 626.
[17] A. Caprani, M. Marie de Ficquelmont-Loizos, L. Tamisier and P. Peronneau, *ibid.* **135** (1988) 635.
[18] D. J. Roha, MS thesis, University of California, Berkeley (1981).
[19] P. J. Sonneveld, W. Visscher, E. Barendrecht, *J. Appl. Electrochem.* **20** (1990) 563.
[20] D. W. Gibbons, R. H. Muller and C. W. Tobias, *J. Electrochem. Soc.* **138** (1991) 3255.
[21] P. K. Andersen, R. H. Muller and C. W. Tobias, *ibid.* **136** (1989) 391.
[22] R. Greef, R. Peat, L. M. Peter, D. Pletcher and J. Robinson, 'Instrumental Methods in Electrochemistry', Ellis Horwood, Chichester (1985), p. 124.
[23] S. Iseki, K. Ohashi and S. Nagaura, *Electrochim. Acta* **17** (1972) 2249.
[24] A. G. C. Kobussen, PhD thesis, University of Utrecht (1981) pp. 44–6.
[25] J. O'M. Bockris, D. Drazic and A. R. Despic, *Electrochim. Acta* **4** (1961) 325.
[26] K. E. Heusler, 'Encyclopedia of Electrochemistry of the Elements', Vol. IX part A, (edited by A. J. Bard), Marcel Dekker, New York (1982), p. 300.